AIAA 93-0575
The Effects of Buoyancy on the Critical Heat Flux in Forced Convection

M. J. Brusstar and H. Merte, Jr.
Department of Mechanical Engineering
and Applied Mechanics
The University of Michigan
Ann Arbor, Michigan

31st Aerospace Sciences Meeting & Exhibit
January 11-14, 1993 / Reno, NV

For permission to copy or republish, contact the American Institute of Aeronautics and Astronautics
370 L'Enfant Promenade, S.W., Washington, D.C. 20024

AIAA-93-0575

THE EFFECTS OF BUOYANCY ON THE CRITICAL HEAT FLUX IN FORCED CONVECTION

Matthew J. Brusstar*
Herman Merte, Jr.**
Department of Mechanical Engineering and Applied Mechanics
The University of Michigan
Ann Arbor, Michigan

ABSTRACT

The critical heat flux (CHF) in forced convection over a flat surface at relatively low flow velocities has been found, not unexpectedly, to depend upon the orientation of the buoyancy. The CHF for R-113 was measured at various heating surface orientations for test section Reynolds numbers ranging between 3000 and 6500. In this flow range, the buoyancy force acting on the vapor generally dominates over the flow inertia, yet the inertia would still be substantial were gravity to be reduced.

In the experiments of this study, the CHF is determined for heating surface orientations ranging from 0° to 360°, for flow velocities between 4 cm/s and 35 cm/s, and for subcoolings between 2.8°C and 22.2°C. The results presented here demonstrate the strong influence of buoyancy at low flow velocities, which diminishes as the flow velocity and subcooling are increased. In addition, a simple model of the effects of varying buoyancy orientation on the CHF in pool boiling is proposed to correlate the CHF at low flow velocities, which finally leads to an analogy between the CHF under adverse buoyancy and that under microgravity.

NOMENCLATURE

ρ_v	density of vapor phase
ρ_l	density of liquid phase
h_{fg}	latent heat of evaporation
σ	surface tension
g	gravitational acceleration
c_{pl}	specific heat of the liquid phase
ΔT_{sub}	subcooling
q_c	CHF
q_z	CHF in saturated pool boiling predicted by Zuber's model
q_{co}	q_z corrected for subcooling
F_{Buoy}	buoyancy force
F_{Drag}	drag force
θ	orientation angle as designated in Figure 5
U_t	terminal velocity
L_c	characteristic length dimension

* - Graduate Research Assistant
** - Professor of Mechanical Engineering

INTRODUCTION

Fundamental to studies in boiling is the critical heat flux (CHF), which represents the upper limit to heat transfer obtainable through nucleate boiling under a given set of conditions. Whereas previous studies of the CHF have concentrated mainly either on pool boiling or on forced convection boiling at high flow velocities, relatively little work has been devoted to the region spanning the interval between these two extremes. In this intermediate region, with which this work is concerned, buoyancy dominates in the case near pool boiling, but its influence wanes with increasing flow velocity.

In applications to power generation and thermal management systems in space, the importance of studying flow boiling at intermediate velocities becomes more apparent. Power consumption by the system must be optimized with respect to its ability to transport heat effectively, which impresses the need for a greater understanding of forced convection boiling with reduced flow velocities. However, the knowledge gained thus far in investigations in this area under earth's gravity applicable to microgravity is rather unsubstantial, due mainly to the difficulty in discerning the effects of the imposed velocity relative to buoyancy. Adding to this are the problems associated with obtaining microgravity or variable gravity for a sustained period of time in the laboratory. The approach that this work has taken to circumvent these problems is to study the effects of varying the orientation of the buoyancy force with respect to the flow velocity, which thus varies its magnitude in the direction of the imposed flow.

Several aspects of pool boiling are retained at relatively low flow velocities. The motion of the vapor is largely governed by buoyancy, and the flow inertia is rather inconsequential in determining the manner in which liquid is resupplied to the heating surface. In the case where the heating surface faces downward, vapor is pinned against the surface by buoyancy, which obstructs the return flow of liquid. A model is proposed in this work which attempts to describe the CHF under such conditions. In this, the mechanisms for dryout may be comparable to those which would be expected for flow boiling in microgravity, given the sliding motion of the void over the surface and the absence of hydrodynamic instabilities.

This study presents the results of the CHF measurements taken for a limited range of orientations, subcoolings, and flow velocities in forced convection boiling over flat, rectangular metal heating surfaces. A model which relates the effects of orientation on the CHF expected for pool boiling is compared with the results at low velocities, with reasonable agreement. As the effects of the flow inertia become more pronounced at the high velocity, however, it will be shown that the dependence of the CHF upon orientation changes significantly.

Copyright c 1993 by the American Institute of Aeronautics and Astronautics, Inc.
All rights reserved.

MODEL DESCRIPTION

The model presented here is a first attempt to characterize the effects of varying the heating surface orientation on the CHF in pool boiling. Because of the many similarities of pool boiling and low velocity forced convection boiling (ref. Katto, 1985), it will be shown that the results of this model may be favorably compared with the experimental CHF data obtained at low velocities. The model is divided into two domains corresponding to upward-facing heating surface orientations and downward-facing ones, each of which is characterized by distinctly different mechanisms.

For upward-facing orientations, where buoyancy acts to carry the vapor away from the surface, vapor jet structures characteristic of the hydrodynamic instability models arise (Lienhard and Dhir, 1973; Zuber, 1958), even with the existence of a forced flow tangent to the surface (Haramura and Katto, 1983). In accordance with the apparent dominance of pool boiling mechanisms, the predicted values of the CHF for all upward-facing orientations should be reasonably close to that predicted by Zuber's model for the CHF over infinite, horizontal flat plates, given as follows:

$$q_z = \frac{\pi}{24}\rho_v h_{fg}\left[\sigma g(\rho_l - \rho_v)/\rho_v^2\right]^{1/4} \tag{1}$$

The influence of bulk liquid subcooling has been incorporated into Equation (1) with a semi-empirical correlation by Ivey and Morris (1962), which bases the effect upon the increase in sensible heat energy necessary to bring the liquid reaching the surface to the saturated state:

$$q_{co} = q_z\left[1 + 0.102\left(\rho_l/\rho_v\right)^{0.75}\frac{c_{pl}\Delta T_{sub}}{h_{fg}}\right] \tag{2}$$

The values for the CHF at various subcoolings based on Equation (2) are given in Table 1.

Subcooling (°C)	q_{co} (W/cm^2)
Sat.	21.8
2.8	23.9
5.6	26.1
11.1	30.3
22.2	38.8

Table 1. CHF values for pool boiling over an infinite, horizontal flat plate.

For downward-facing orientations, a different CHF model must be constructed to account for the effects of adverse buoyancy on the vapor removal and liquid replenishment at the surface. While previous studies of pool boiling (Haramura and Katto, 1983) suggest the existence of jet-like vapor structures even in the presence of adverse buoyancy, this seems unlikely in light of the tendency of the jets to collapse upon themselves under such conditions. In the present study the vapor was observed to slide along the heating surface, pressed against it under the action of buoyancy. Given this observation, an appropriate model of the CHF can be constructed based upon the obstruction of enthalpy flow to the surface caused by the sliding vapor mass. This concept is similar to that in the model presented by Weisman and Pei (1983) for low-quality forced convection boiling, except that the motion at the surface is governed by buoyancy in the present case instead of by the flow inertia. As such, enthalpy is transported to the heating surface through entrainment behind the departing vapor, which effectively pumps the liquid from the bulk liquid region in a direction assumed to be tangent to the heater surface. Thus, it should be expected that the CHF will depend upon the velocity at which liquid is supplied to the surface, which may be approximated by the terminal velocity of the vapor. Assuming the viscosity of the vapor to be small and that dryout occurs only at the CHF, so that the vapor slides along atop a thin liquid film, then viscous and solid-liquid-vapor surface tension effects can be neglected. The resulting balance of buoyancy and drag forces in the direction of fluid motion, shown in Figure 1, yields the terminal velocity in Equation (3):

$$\begin{aligned} F_{Buoy} &= F_{Drag} \\ g\sin\theta(\rho_l - \rho_v)L_c^3 &\sim \rho_l U_t^2 L_c^2 \\ U_t &= \pm C|\sin\theta|^{1/2} \end{aligned} \tag{3}$$

where C is then a function of g, of some characteristic dimension for the vapor, and of the densities of the liquid and vapor. Considering that the CHF approaches the predicted value for upward-facing orientations for the two extremes of this domain, $\theta = 90°$ and $270°$, the following relationship is obtained for downward-facing orientations in pool boiling:

$$q_c = q_{co}|\sin\theta|^{1/2} \tag{4}$$

where q_{co} is defined by Equation (2), and q_c is the CHF. This result, combined with that for upward-facing orientations, is compared below with experimental data.

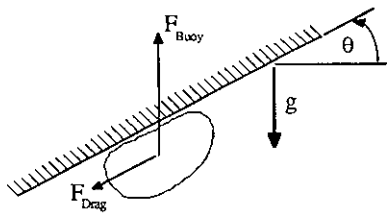

Figure 1. Forces acting on a vapor mass under adverse buoyancy.

EXPERIMENTAL APPARATUS

The experiments were conducted in a forced convection loop shown schematically in Figure 2. Generally, the loop provides for the controlled variation of four main parameters at the test section: temperature, subcooling, flow velocity (or mass flux), and orientation with respect to gravity. Automatic control schemes are utililized for maintaining the temperature, subcooling, and flow velocity of the bulk liquid at the entrance of the test section to the desired levels. The entire loop can be rotated about its center of gravity, as shown, and fixed at any orientation between 0° and 360°. The salient features of the loop are described below.

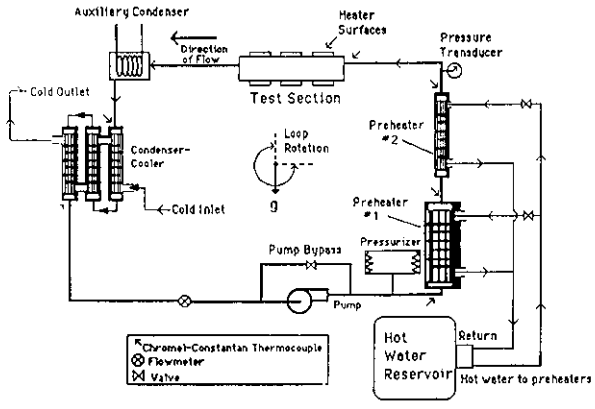

Figure 2. Forced convection loop.

R-113 flows through the loop at a set rate determined by the speed of a DC-driven centrifugal pump, which is controlled by an electrical feedback loop linked to a microprocessor. This arrangement provides the capability for varying the volume flow rate over a ratio of nearly 10:1, with a maximum output of approximately 7.5 liters/min.

The pressure in the loop is maintained within about ±0.025 psi of its set point by means of a pneumatically-controlled stainless steel bellows. The set point is adjusted to provide the desired level of subcooling in the test section for the prescribed liquid temperature.

Two preheaters at the pump exit are used to raise the temperature of the R-113 at the inlet to the test section to the level desired, between 25°C (77°F) and 60°C (140°F). Preheater #1 raises the bulk liquid temperature close to the desired level, while preheater #2 is then adjusted so that the measured inlet temperature reaches the desired value to within about ±0.06°C (0.1°F). Both preheaters receive hot water from a controlled constant-temperature reservoir at a flow rate varied by an electronic controller to obtain the desired test section inlet temperature, which is measured and fed back to the controller.

The test section is shown in greater detail in Figure 3, and consists of a rectangular duct, 10.5 cm (4-1/8") wide by 35.6 cm (14") long. The height may be selected from three available sections to be 3.2 mm (1/8"), 12.7 mm (1/2") or 25.4 mm (1"), which permits varying the bulk velocity by more than a factor

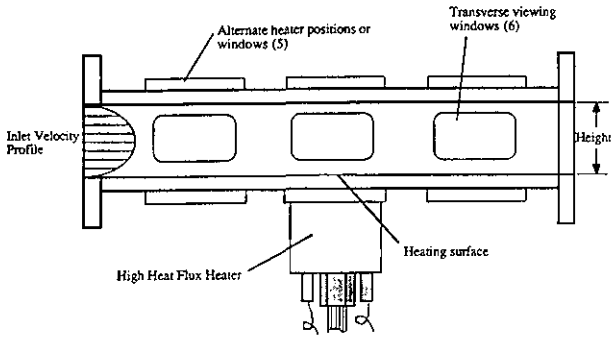

Figure 3. Test section.

of thirty with the existing pump. Under maximum flow conditions, the Reynolds number based on hydraulic diameter for these test sections with R-113 is about 6500. On the sides and opposite the test surface are optical-grade quartz windows which allow for transverse as well as overhead views of the heater surface during operation.

A condenser-cooler following the test section acts to prevent cavitation at the pump inlet. Heat is removed from the loop through a counterflow shell-and-tube heat exchanger to a water-cooled reservoir. Cold water may also be circulated through the auxiliary condenser as necessary to aid in the removal of excess latent heat energy during CHF tests at low subcoolings.

The heater surface used for these experiments is shown in Figure 4, and was designed to provide heat flux levels up to 80 W/cm^2. The heater consists of a copper body heated by three cartridge heaters in its base and insulated on all sides to provide a large heat capacity and uniformity of temperature at the boiling surface. Three chromel-constantan (type E) thermocouples are placed at precise locations beneath one another in the straight section leading to the upper surface so that the surface heat flux and temperature can be calculated. A smooth copper foil 0.1 mm (0.004 in.) thick was soldered over

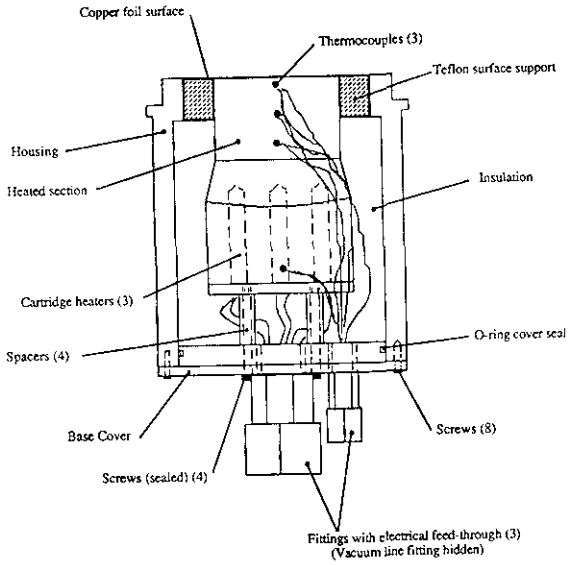

Figure 4. High heat flux copper heater.

the top surface so as to prevent boiling at the crevices around the surface perimeter and in grooves on the surface produced by machining. The heating surface is rectangular in shape, 1.91 x 3.81 cm (0.75 x 1.50 in.), and is flat to eliminate any surface tension curvature effects and to maintain a constant orientation between the body force and the heater surface.

Before filling the flow loop, the R-113 is degassed and purified in a multistep process in order to remove any impurities which might otherwise promote nucleation artificially. The purity of the fluid was verified through measurements of the vapor pressure under quasi-steady saturated conditions, which justifies the use of the thermodynamic property tables in the data analysis.

EXPERIMENTAL PROCEDURES

Prior to placement in the flow loop, each test surface was calibrated in air to determine the amount of heat lost to the surroundings as a function of the temperature at the base of the heater. Thus, the amount of heat supplied to the heater surface can be calculated by measuring the power input to the heater and subtracting the peripheral heat losses estimated from the measured base temperature.

The flow boiling experiments were conducted by first setting the orientation, flow velocity, pressure, and temperature in the loop to their desired values. Approximately four hours were allowed for the flow loop to reach steady state operating conditions before commencing testing. Nucleate boiling was initiated on the surface at a heat flux known to be far below the CHF as a precaution against a sudden jump into the film boiling region. Once quasi-steady nucleate boiling had been attained, the voltage across the heater terminals was raised in an incremental fashion, allowing the surface to reach a quasi-steady temperature at each step. The inlet temperature to the test section, the pressure in the loop, the flow rate, the temperature measurements in the heater, and the input voltage and current were then recorded before moving to the next higher increment.

The CHF was defined as that heat flux level above which a sudden or gradual temperature excursion at the heater surface was observed, which caused a safety relay to open the heater circuit. The last recorded quasi-steady operating point prior to this event is subsequently used to calculate the CHF.

The various orientations used for these experiments are defined with respect to the horizontal upward position, as shown in Figure 5. The orientation was varied to change the direction of the buoyancy force relative to both the imposed flow velocity and the heater surface. The reference position,

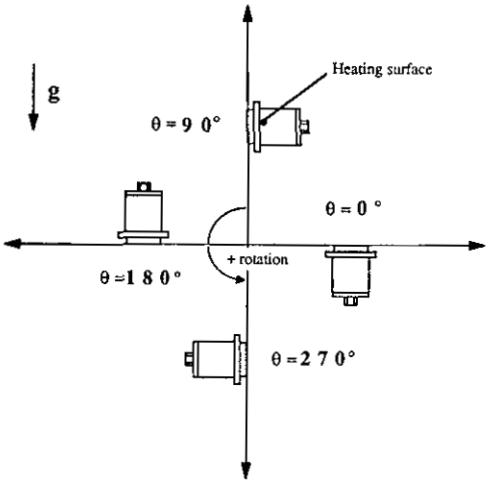

(Arrows indicate the direction of flow over the heating surface)

Figure 5. Orientation angle designations.

with the surface horizontal and facing upward, with the body force therefore normal to the flow direction, is called 0° or 360°. The other orientations are then defined by setting the direction of rotation such that the vertical upflow position corresponds to an angle of $\theta = 90°$. As such, the horizontal facing downward position corresponds to $\theta = 180°$ and the vertical downflow position with $\theta = 270°$. The variation of the direction of the buoyancy force associated with the change in orientation is responsible for the effects to be demonstrated in the following section.

RESULTS

The results presented below are measurements of the CHF for R-113 with quasi-steady heating for various orientations at different flow velocities and subcoolings. The effects of orientation on the CHF are considered first at low bulk velocities, where buoyancy is observed to largely dominate, as in pool boiling. A comparison is then made between this data and the results from the model discussed earlier in this work, which includes the effect of subcooling. Measurements of the CHF for a higher flow velocity then will be presented, which illustrate the effect of increasing flow momentum, as well as a dependence upon void fraction related to the geometry of the test section.

Low flow velocities (4 cm/s and 8.5 cm/s)

Figure 6 shows the effect of orientation on the CHF, which is non-dimensionalized with respect to the corresponding subcooled pool boiling CHF values taken from Table 1. The flow velocity was 4 cm/s, and the subcooling was 2.8°C, 5.6°C and 11.1°C. For upward-facing orientations ($\theta = 0°$ to 90°, and 270° to 360°), the calculated CHF values agree reasonably with the model, with only a slight enhancement attributable to the forced flow. The strong dominance of buoyancy over the flow momentum is illustrated clearly at the downward-facing orientations ($90° < \theta < 270°$), where the CHF decreases sharply to a minimum of nearly 0 W/cm^2 as the orientation approaches 180°. In this case, dryout of the heater surface was observed to occur near boiling inception, since the imposed flow velocity was insufficient to remove the vapor

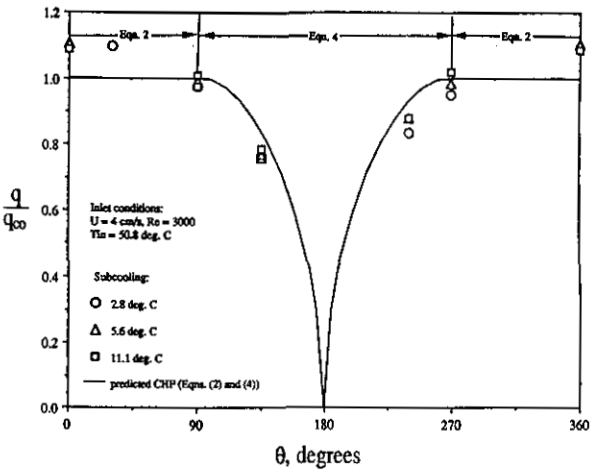

Figure 6. CHF versus orientation angle, U = 4 cm/s.

held against the surface by buoyancy. For all of the orientations at this flow velocity, the velocity of the vapor induced by buoyancy was observed to prevail over that of the bulk liquid flow.

The effect of subcooling at the low velocity, which is incorporated in the non-dimensionalization, shows good agreement with the subcooling correlation expressed in Equation (2) for both upward- and downward-facing orientations. Although visual observations suggest different mechanisms for the CHF between upward- and downward-facing orientations, the effects appear to be uniformly well-correlated by the model equation.

Figure 7 shows the CHF plotted as a function of orientation for an imposed flow velocity of 8.5 cm/s. As in the previous figure, the data appear to agree well with the proposed model, indicating again the predominance of buoyancy relative to the inertia of the imposed flow. Similar to the lowest flow velocity, the buoyancy acting on the vapor appears to dominate over the flow inertia at every orientation, including the horizontal facing downward position (180°). A comparison of the CHF for the upward-facing orientations with the pool boiling model shows only a modest increase attributable to the momentum of the imposed flow. Perhaps more telling, however, is a comparison of the CHF at the two vertical orientations, 90° and 270°, where upflow and downflow exist, respectively. The two values are nearly identical, indicating very little effect associated with the flow inertia.

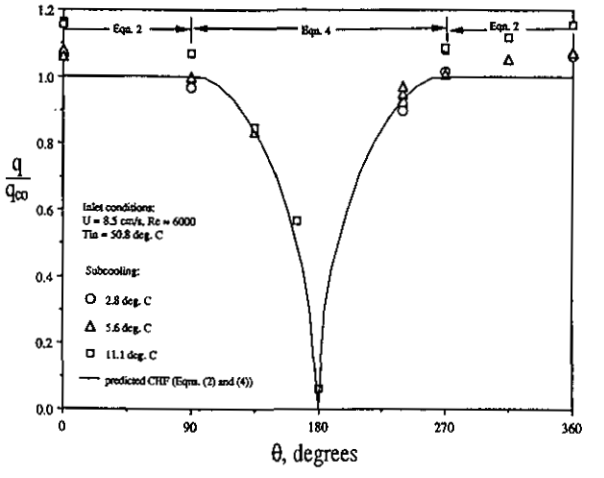

Figure 7. CHF versus orientation angle, U = 8.5 cm/s.

The effect of subcooling in Figure 7 is similar to that observed in Figure 6. The data points are correlated very well, once again, by the model equation.

High flow velocity (35 cm/s)

Figure 8 shows the results for the highest velocity, 35 cm/s, non-dimensionalized for subcoolings of 5.6°C, 11.1°C, and 22.2°C. CHF tests at lower subcoolings were not possible in the existing experimental facility due to the immense amount of void generated at the heater surface, which interfered with the proper functioning of the flow loop. In this figure, the

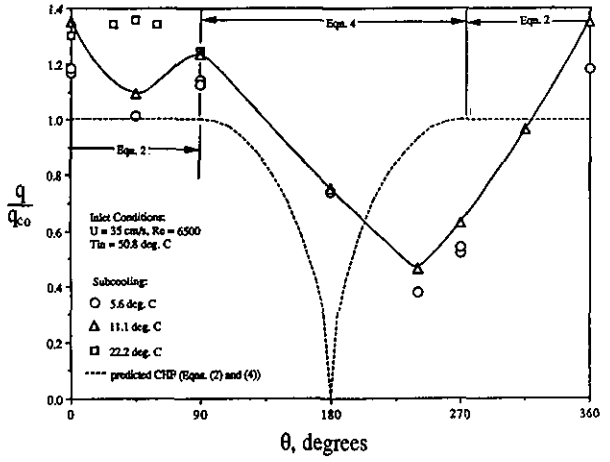

Figure 8. CHF versus orientation angle, U = 35 cm/s.

effect of flow inertia is observed to be rather substantial, as the dramatic difference of the CHF values for vertical upflow (90°) and vertical downflow (270°) illustrate. Also, this figure differs strikingly from the two previous ones in that the minimum CHF is significantly greater than zero and occurs at a downward-facing orientation inclined with buoyancy against the direction of flow, at 240°. Also of note is the sag in the curve near 45° at the two lower subcoolings, which evidently does not exist at the highest subcooling of 22.2°C. This effect quite likely is the result of the interference of the plate opposite the heater surface on the departing vapor masses. The data for the highest subcooling suggests that, in the absence of the excessive void fraction brought about by the confined geometry, the maximum CHF for the lower subcoolings would also occur at an orientation of approximately 45°, where the surface is facing upward and is inclined with buoyancy in the direction of the flow.

Unlike the lower velocity cases of Figure 6 and 7, the subcooling model used does not correlate the data well at the higher velocity in Figure 8. The CHF is decreased disproportionately as the subcooling is decreased, relative to the data presented in Figures 6 and 7. Especially noteworthy is the effect at 45°, where an increase in subcooling from 11.1°C to 22.2°C changed the characteristic relationship between the CHF and orientation seen at the lower subcoolings. At the highest subcooling, the void volume present above the heating surface was notably reduced from that at the lower subcoolings.

DISCUSSION

Relatively few studies concerning the effects of buoyancy on the CHF in forced convection exist with which the results of the previous section may be compared. However, as the data of the previous section showed, much of what was observed at the lower velocities is better described by pool boiling mechanisms. Even for the case of pool boiling, though, the results with adverse buoyancy in particular require some interpretation.

The success of the hydrodynamic model exhibited at the low flow velocities is not surprising for the upward-facing orientations (θ from 0° to 90° and 270° to 360°), since the motion of the vapor departing the surface appeared be largely unaffected by the imposed flow. For the downward-facing orientations (θ from 90° to 270°), however, the void tended to slide over the surface, which thus lowered the CHF. This decreasing effect may be attributed to several factors. First, the nearly static vapor mass existing above the surface under these conditions blocks much of the exchange of enthalpy with the bulk liquid region, and the CHF occurs upon dryout of the thin liquid layer remaining beneath the vapor at the surface. A similar mechanism for the CHF was noted previously by Tong and Hewitt (1972) for flow boiling at low velocities and lower subcoolings, under conditions of slug flow. Secondly, the effect of excessive vapor production resulting from the increased contact area between the vapor and heated surface and from thin film evaporation beneath the vapor tends to exacerbate the obstruction of the liquid inflow to the heater surface. This effect is reported in the work of Fujita, et al. (1988) for pool boiling, where the CHF is shown to decline substantially as the surface is rotated toward the horizontal facing downward position.

The effect of subcooling at low velocities seems to correlate fairly well with the correlation given earlier in the model description, though the physical means which produce this result likely differs between downward-facing and upward-facing orientations. Regardless of whether this effect is the result of condensation of the departing vapor, as suggested by Zuber, et al. (1961), or by the additional heat energy needed to bring the subcooled liquid to the saturated state (Kutateladze, 1963), the resulting correlation will take nearly the same form as Equation (2). For downward-facing orientations, where the CHF results upon dryout of a liquid film, the subcooling effect will be like that described by Kutateladze. For the CHF at upward-facing orientations (θ from 0° to 90° and 270° to 360°), which results from hydrodynamic instability, condensation likely is the predominant effect. Regardless of the means by which subcooling affects the process, the data presented here for low velocities suggest that a similar model of subcooling effects may be used at all orientations with reasonable accuracy.

The effect of flow velocity in Figures 6 and 7 appears to be rather small, owing much to the fact that the buoyant velocity was predominant over that of the imposed flow. As the flow inertia was increased, however, Figure 8 shows that there results a significant departure from pool boiling. While the vapor was still observed to slide along the surface for the downward-facing orientations at the high flow velocity, its motion was markedly influenced by the forced flow. As a result, the CHF at the high velocity was not so dramatically affected by the adverse buoyancy of the horizontal downward position (180°), even though a general decreasing trend in the data is seen for downward-facing orientations. Papell (1966) studied the relative effects of buoyancy and flow momentum by comparing the CHF in vertical tubes for the cases of upflow and downflow. The results presented were divided into buoyancy-dependent and buoyancy-independent flow regimes, which were functions of the flow velocity, subcooling and system pressure. The dependence upon buoyancy was said to have been brought about by an accumulation of void resulting from the balance of buoyancy and drag forces, an effect which was mitigated as the flow inertia was increased. An earlier visual study by Simoneau and Simon (1966) in a similar configuration affirms these assertions. A comparison of the two vertical orientations, θ = 90° and 270°, in Figure 8 also exhibits the same phenomenon. Indeed, visual observations at the CHF with downflow showed a congregation of vapor bubbles above the surface as a result of the near balance of inertia and buoyancy forces, which consequently resulted in a lower CHF.

The effect of subcooling exhibited in Figure 8 appears to be a bit more complex than that for the lower flow velocities, as witnessed by the relatively poor correlation of the data with equation (2). The difference in this case is that the CHF was adversely affected by the excessive void volume produced by the heater, which increases with decreasing subcooling. This effect is certainly intensified by the relatively narrow test section height (3.2 mm) used for the high velocity experiments. The most striking example of this occurs at $\theta = 45°$, where the decrease in the CHF between 0° and 90° at lower subcoolings disappears as the subcooling is raised to 22.2°C. A similar effect of void fraction was noted by Papell and Simoneau and Simon in the works cited above, where an increase in subcooling decreased the accumulation of void near the surface, which thereby reduced the adverse effects on the CHF associated with downflow.

In the downward-facing orientations, where the departing vapor is observed to slide along the surface, and where there is an absence of unstable hydrodynamic phenomena, an analogy between this condition and that in forced convection in microgravity can be drawn. In pool boiling in microgravity, it has been observed by Ervin (1991) that the vapor remains stationary upon the heating surface following the point of boiling inception. In the presence of an imposed flow of liquid, it is expected that the vapor should slide along the surface, and that the mechanism for the CHF would be the evaporation of the thin liquid film existing beneath the vapor. Under conditions of adverse buoyancy, the same mechanism dominates, much as if conditions of slug flow prevailed. The heat flux at which dryout of the film occurs depends on the rate at which the film is replenished, and on the subcooling of the incoming liquid; the film thickness will be independent of buoyancy (Bankoff, 1990). So, the motion of the vapor, whether driven by the inertia of the imposed flow or by buoyancy, will determine the rate at which the film is replenished, and thus will govern the CHF. In this way, the mechanism of the CHF for downward-facing orientations under earth's gravity can be seen as similar to those which would exist in forced convection boiling in microgravity. For example, in the case where there is no motion of the vapor at the heating surface, as with the horizontal down position at low flow velocities and with pool boiling in microgravity, the data presented here and by Ervin show that the CHF occurs at heat flux levels approaching zero. When buoyancy induces motion of the departing vapor, as predicted by Equation (3), the CHF rises in a manner which may be predicted by mechanisms similar to those existing in forced convection in microgravity.

CONCLUSIONS

Based on the results obtained thus far in this study of the effects of buoyancy on the CHF, the following conclusions are drawn:

1. Buoyancy dominates the CHF mechanisms at low flow velocities, much as in pool boiling. The role that the forced flow inertia would otherwise play in the absence of gravity is thus obscured, and it is seen to have only a modest effect on the CHF in these experiments.

2. Except in cases of excessive void fraction, as observed in the experiments at the high velocity, the effects of subcooling may be attributed to the increased contribution of sensible heat energy. A correlation based on this assumption was used with good success.

3. The CHF at downward-facing orientations seems to be determined mainly by the rate at which liquid is fed to the heating surface by means of entrainment behind the departing vapor. An analogy can be drawn between this condition and that which would exist in forced convection boiling in microgravity.

Acknowledgement - This work was supported in part under NASA Grant NAG3-589.

REFERENCES

Bankoff, S. G., 1990, "Dynamics and Stability of Thin Heated Liquid Films", *J. Heat Transfer*, v. 112, pp. 538-546.

Ervin, J. S., 1991, "Incipient Boiling in Microgravity", Ph. D. Thesis, Dept. of Mech. Eng., University of Michigan.

Fujita, Y., Ohta, H., Uchida, S., Nishikawa, K.,1988, "Nucleate Boiling Heat Transfer and Critical Heat Flux in Narrow Space Between Rectangular Surfaces, *Int. J. Heat Mass Transfer*, v. 31, n. 2, pp. 229-239.

Haramura, Y., Katto, Y., 1983, "A New Hydrodynamic Model of Critical Heat Flux, Applicable to Both Pool and Forced Convection Boiling on Submerged Bodies in Saturated Liquids", *Int. J. Heat Mass Transfer*, v. 26, n. 3, pp. 389-399.

Ivey, H. J., Morris, D. J., 1962, "On the Relevance of the Vapour-Liquid Exchange Mechanism for Subcooled Boiling Heat Transfer at High Pressure", UKAEA, AEEW-R 137.

Katto, Y., 1985, "Critical Heat Flux", *Adv. in Heat Transfer*, v. 17, pp. 1-64.

Kirk, K. M., 1992, "A Study of the Relative Effects of Buoyancy and Liquid Momentum in Forced Convection Nucleate Boiling", Ph. D. Thesis, Dept. of Mech. Eng., University of Michigan.

Kutateladze, S. S., 1963, "Fundamentals in Heat Transfer", p. 387, Arnold, London.

Lienhard, J. H., Dhir, V. K., 1973, "Hydrodynamic Prediction of Peak Pool-Boiling Heat Fluxes from Finite Bodies", *Trans. ASME, Ser. C, J. Heat Transfer*, v. 95, pp. 152-158.

Papell, S. S., 1967, "Buoyancy Effects on Forced-Convective Boiling", ASME Report 67-HT-63.

Simoneau, R. J., Simon, F. F., 1966, "A Visual Study of Velocity and Buoyancy Effects on Boiling Nitrogen", NASA TN D-3354.

Tong, L. S., Hewitt, G. F. , 1972, "Overall Viewpoint of Flow Boiling CHF Mechanisms", ASME Paper 72-HT-54.

Weisman, J., Pei, B. S., 1983, "Prediction of the Critical Heat Flux in Flow Boiling at Low Qualities", *Int. J. Heat Mass Transfer*, v. 26, n. 10, pp. 1463-1477.

Zuber, N., 1958, "On the Stability of Boiling Heat Transfer", *Trans. of the ASME*, v. 80, pp. 711-720.

Zuber, N., Tribus, M., Westwater, J. W., 1961, "The Hydrodynamic Crisis in Pool Boiling of Saturated and Subcooled Liquids", *International Developments in Heat Transfer*, p. 230, ASME, New York.